

CHAPTER-2

EXPERIMENTAL

The purpose of the present investigation was to study the corrosion inhibition behavior of heterocyclic inhibitors in 1M HCl using weight loss, electrochemical, surface and computational methods.

2.1. Materials

2.1.1. Test Material

For all weight loss, electrochemical experiments, and surface studies the mild steel specimens were cut from the commercially available mild steel sheet having chemical composition (weight percentage): C (0.076), Mn (0.192), P (0.012), Si (0.026), Cr (0.050), Al (0.023), and Fe (balance). The exposed surface of the working electrodes was cleaned successively with emery papers of different grade (600, 800, 1000, 1200), washed with deionized water, degreased with acetone, ultrasonically cleaned with ethanol and stored in moisture free desiccator before used in the experiments.

2.1.2. Test solution

Test solution was 1M HCl for weight loss, electrochemical and surface measurement which was prepared by dilution of an analytical reagent grade 37% HCl in double deionized water.

2.1.3. Chemicals

Chemical used in the present study was purchased from Merck, HiMedia, Qualigens, Loba-Chemie, and SDFCL chemical manufacturers. These chemicals were of 98 to 100% purity and used for synthesis of several heterocyclic inhibitors used in the present study without any further purification.

2.2. Heterocyclics inhibitors

In the present investigation all thirteen inhibitors were synthesized according to the previously reported methods. The corrosion inhibition behavior of these thirteen inhibitors has been discussed in four sections:

A. 5-arylpyrimido-[4, 5-b] quinoline-diones (APQDs)

- (1) 5-(4-nitrophenyl)-5,10-dihydropyrimido [4,5-b]quinoline-2,4(1H,3H)-dione
(APQD-1)
- (2) 5-phenyl-5,10-dihydropyrimido[4,5-b]quinoline-2,4(1H,3H)-dione (APQD-2)
- (3) 5-(4-hydroxyphenyl)-5,10-dihydropyrimido[4,5-b]quinoline-2,4(1H,3H)-dione
(APQD-3)
- (4) 5-(2,4-dihydroxyphenyl)-5,10-dihydropyrimido[4,5-b]quinoline-2,4(1H,3H)-
dione (APQD-4)

B. 2-amino-4-arylquinoline-3-carbonitriles (AACs)

- (5) 2-amino-4-(4-nitrophenyl) quinoline-3-carbonitrile(AAC-1)
- (6) 2-amino-4-phenylquinoline-3-carbonitrile (AAC-2) and
- (7) 2-amino-4-(4-hydroxyphenyl) quinoline-3-carbonitrile (AAC-3)

C. 2, 4-diamino-5-(phenylthio)-5H-chromeno [2, 3-b] pyridine-3-carbonitriles (DHPCs)

- (8) 2,4-diamino-7-nitro-5-(phenylthio)-5H-chromeno[2,3-b]pyridine-3-carbonitrile
(DHPC-1)
- (9) 2,4-diamino-5-(phenylthio)-5H-chromeno[2,3-b]pyridine-3-carbonitrile (DHPC-
2)
- (10) 2,4-diamino-7-hydroxy-5-(phenylthio)-5H-chromeno[2,3-b]pyridine-3-
carbonitrile (DHPC-3)

D. 3-amino alkylated indoles (AAIs)

(11) N-((1H-indol-3-yl)(phenyl)methyl)-N-ethylethanamine (**AAI-1**)

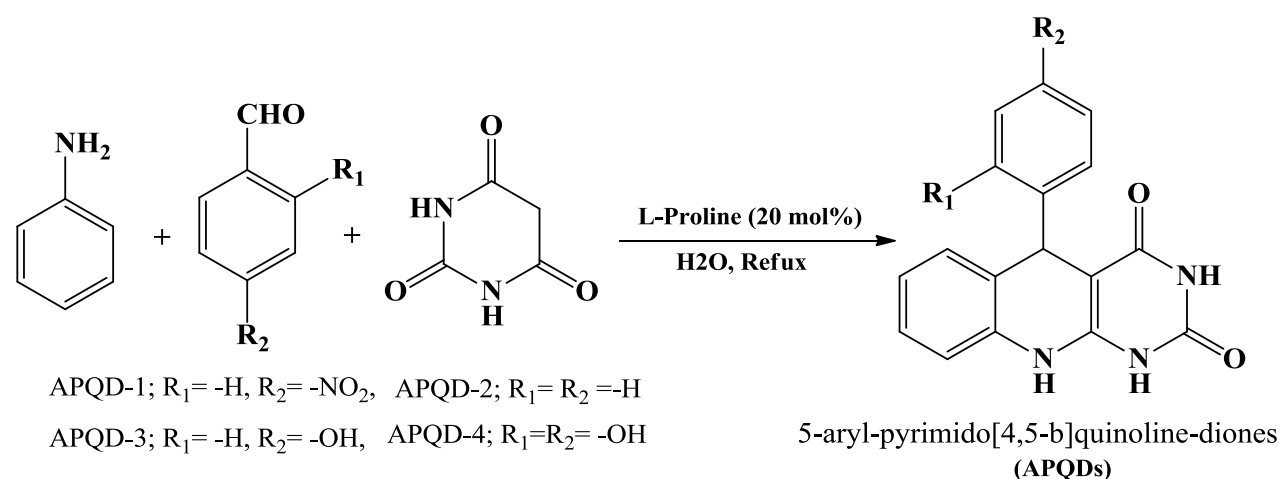
(12) 3-(phenyl(pyrrolidin-1-yl)methyl)-1H-indole (**AAI-2**)

(13) 3-(phenyl(piperidin-1-yl)methyl)-1H-indole (**AAI-3**)

2.2.1: 5-arylpyrimido-[4, 5-b] quinoline-diones (APQDs)

As described in literature[Nezhadet *al.* (2012)], a mixture comprising of aniline (1 mmol), aldehyde (1 mmol), barbutyric acid (1 mmol), and L-proline catalyst (0.05 g, 20 mol %) in water (2 mL) was refluxed for 12 h. The completion of reactions and formation of products were checked by TLC method. After completion of reaction, the reaction mixtures were cooled to room temperature and the resulting solid crude products were filtered. The solid crude precipitates were washed with water (10 mL) and finally with ethanol (5 ml) to obtain pure 5-arylpyrimido-[4,5-b] quinoline-diones (APQDs). The synthesized inhibitors were characterized by physical and spectroscopic analysis. The characterization data of the synthesized compounds are given in Table 2.1. The synthetic scheme for the studied APQDs is shown in scheme 1.

Scheme 1:



Synthetic route of studied APQDs

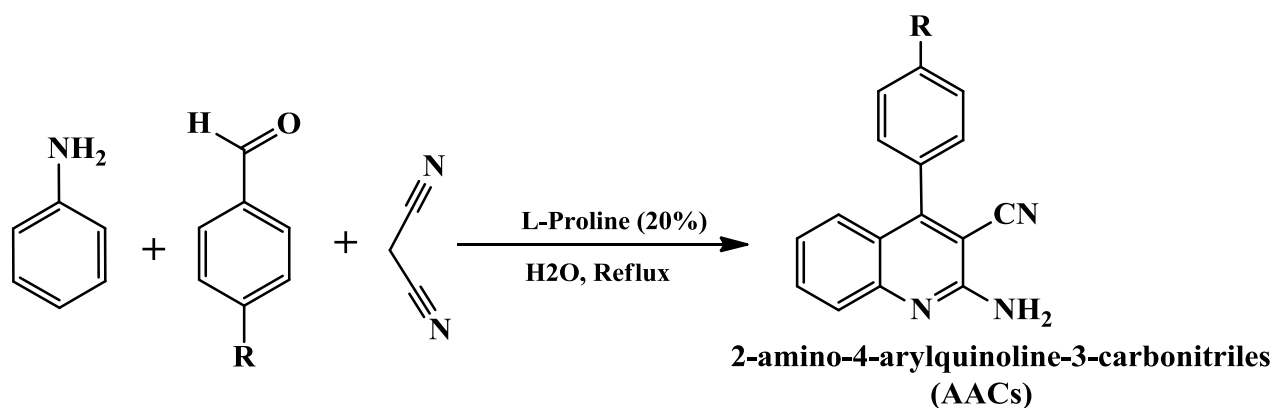
Table 2.1: IUPAC name, molecular structure, molecular formula, melting point and analytical data of studied APQDs

IUPAC name And abbreviation	chemical Structure	molecular formula and analytical data
5-(4-nitrophenyl)- 5,10- dihydropyrimido[4,5- b]quinoline- 2,4(1H,3H)-dione (APQD-1)		C ₁₇ H ₁₂ N ₄ O ₄ (mol. wt. 336.30), IR spectrum (KBr cm ⁻¹): 3556, 3448, 3427, 2842, 1694, 1646, 1536, 1422, 1328, 1093, 858, 624; ¹ H NMR (300 MHz, DMSO-d ₆) δ (ppm): 6.12, 7.22, 7.37-7.43, 7.96-8.07, 10.23-10.42.
5-phenyl-5,10- dihydropyrimido[4,5- b]quinoline- 2,4(1H,3H)-dione (APQD-2)		C ₁₇ H ₁₃ N ₃ O ₂ (mol. wt. 291.30), IR spectrum (KBr cm ⁻¹): 3687, 3574, 3454, 3024, 1680, 1646, 1436, 1402, 1298, 1226, 1163, 786, 742, 718, 628; ¹ H NMR (300 MHz, DMSO-d ₆) δ (ppm): 5.96-6.21, 6.96, 7.11-7.23, 7.54, 8.09, 9.45, 10.83-10.92.
5-(4- hydroxyphenyl)- 5,10- dihydropyrimido[4,5- b]quinoline- 2,4(1H,3H)-dione (APQD-3)		C ₁₇ H ₁₃ N ₃ O ₃ (mol. wt. 307.30), IR spectrum (KBr cm ⁻¹): 3785, 3678, 3582, 1686, 1571, 1456, 1270, 1204, 1168, 1098, 966, 872, 784, 698; ¹ H NMR (300 MHz, DMSO-d ₆) δ (ppm): 5.46, 6.73-6.82, 7.67, 7.96, 8.36, 9.42, 10.76, 12.04-12.13.
5-(2,4- dihydroxyphenyl)- 5,10- dihydropyrimido[4,5- b]quinoline- 2,4(1H,3H)-dione (APQD-4)		C ₁₇ H ₁₃ N ₃ O ₄ (mol. wt. 323.30), IR spectrum (KBr cm ⁻¹): 3843, 3762, 3549, 3428, 2864, 1669, 1627, 1542, 1484, 1436, 1254, 1198, 1045, 958, 679, 624; ¹ H NMR (300 MHz, DMSO-d ₆) δ (ppm): 5.36, 6.59, 6.98-7.11, 7.43, 7.96, 8.56, 9.71, 12.45-12.54.

2.2.2: Synthesis of 2-amino-4-arylquinoline-3-carbonitriles (AACs)

As reported in literature[Nezhadet *al.* (2012)], the investigated 2-amino-4-arylquinoline-3-carbonitriles (AACs) were synthesized by refluxing a mixture comprising of aniline (1mmol), aldehyde (1 mmol), and malononitrile (1 mmol) and L-proline catalyst (0.05 g, 20 mol %) in water (2 mL) was refluxed for 12 h. The synthetic scheme of the investigated AACs is shown in Scheme 2. Completion of reactions and formation of products were checked by TLC method. After completion of reaction, the reaction mixtures were cooled to room temperature and solid crude products were filtered. The solid crude precipitates were washed with water (10 mL) and finally with ethanol (5 ml) to obtain pure AACs. The synthesized inhibitors were characterized by spectroscopic analysis. The chemical structures, IUPAC name, abbreviation and analytical data of the investigated inhibitors are given in Table 2.2. The stock solution of inhibitors was prepared in 1M HCl containing 2% acetone.

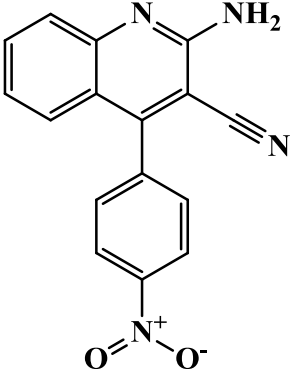
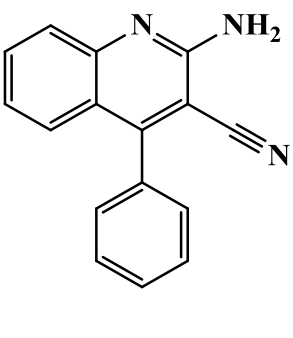
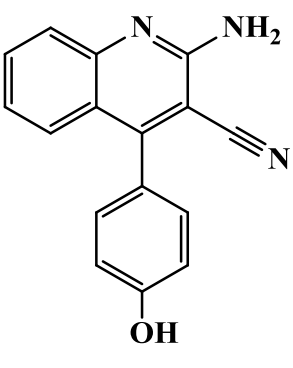
Scheme 2:



AAC-1; -R = -NO₂, AAC-2; -R = -H AAC-3; -R = -OH

Synthetic rout of studied AACs

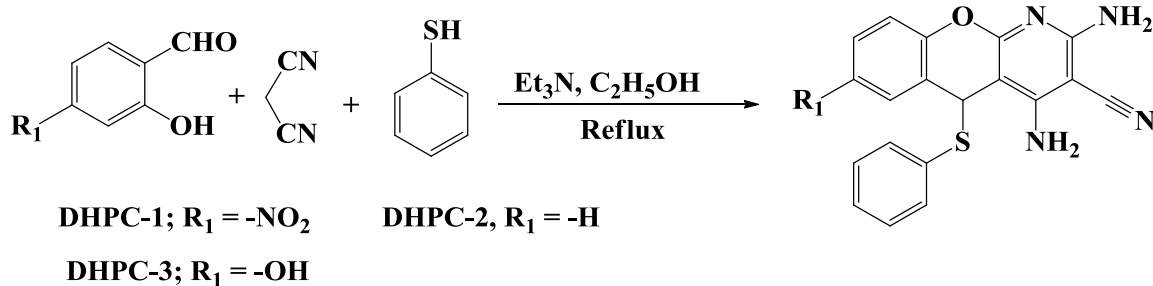
Table 2.2: IUPAC name, molecular structure, molecular formula, melting point and analytical data of studied AACs

IUPAC name and abbreviation of Inhibitor	chemical Structure	molecular formula and analytical data
2-amino-4-(4-nitrophenyl)quinoline-3-carbonitrile (AAC-1)		$C_{16}H_{10}N_4O_2$ (mol. wt. 290.08) Cream colored solid, IR spectrum (KBr cm^{-1}): 3578, 2858, 2228, 1723, 1680, 1656, 1530, 1448, 1357, 1118, 948, 875, 654, 1H NMR (300 MHz, DMSO- d_6) δ (ppm): 6.439-6.627, 6.737-6.763, 7.523- 7.848, 8.031,
2-amino-4-phenylquinoline-3-carbonitrile (AAC-2)		$C_{16}H_{11}N_3$, (mol. Wt. 245.09), Brown colored waxy solid, IR spectrum (KBr cm^{-1}): 3587, 3428, 2871, 2224, 1643, 1503, 1423, 1341, 1154, 924, 735, 652 1H NMR (300 MHz, DMSO- d_6) δ (ppm): 6.337-6.527, 6.462-6.635, 7.338-7.536.
2-amino-4-(4-hydroxyphenyl)quinoline-3-carbonitrile (AAC-3)		$C_{16}H_{11}N_3O$, (mol. wt. 261.09), yellow colored; IR spectrum (KBr cm^{-1}): 3646, 3542, 2856, 2245, 1646, 1564, 1472, 1227, 923, 830, 627 1H NMR (300 MHz, DMSO- d_6) δ (ppm): 6.468-6.725, 6.635-6.974, 7.896-7.938, 8.323

2.2.3: Synthesis of 2, 4-diamino-5-(phenylthio)-5H-chromeno [2, 3-b] pyridine-3-carbonitriles (DHPCs)

The chromenopyridines used in the present study were synthesized by one step multicomponent reactions (MCRs) as previously described [Evdokimov *et al.* (2007)] and the synthetic route is shown in Scheme 3. The progress of reaction was checked by TLC method. After completion of reaction, the products were dissolved in DMF and undissolved components were removed through filtration. Addition of water to DMF results in the crystallization of pure product. The characterization data of the synthesized compounds are given in Table 2.3.

Scheme 3:



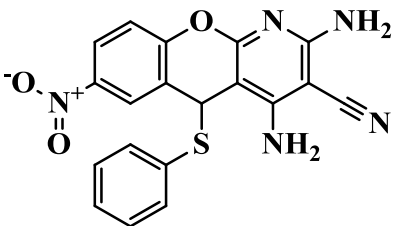
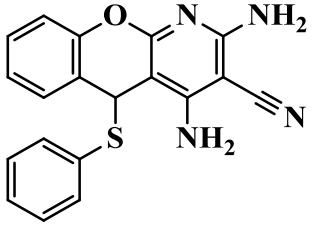
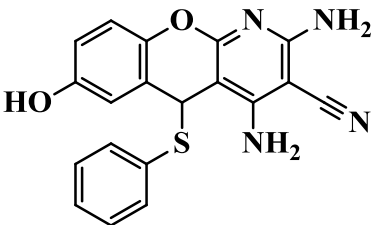
Synthetic route of the studied DHPCs

2.2.4: Synthesis of D.3-amino alkylated indoles (AAIs)

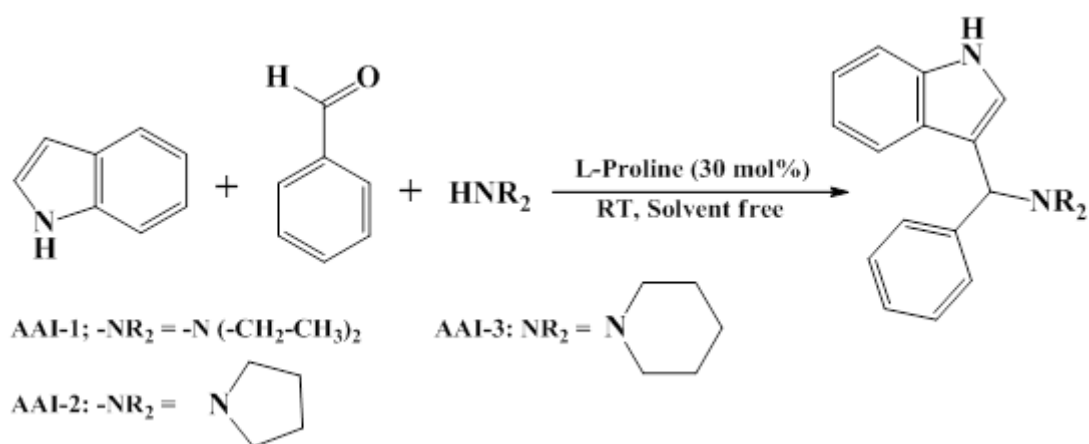
3-amino alkylated indoles (AAIs) used in the present study were synthesized by the method described earlier [Kumar *et al.* (2012)]. In a typical experimental procedure, 1 mmol of the aldehyde, 1 mmol of the secondary amine, 1 mmol indole and 30 mol% of the L proline were placed in a round-bottom flask and stirred at room temperature. The progress and completion of the reaction was monitored by TLC method. After completion of the reaction, the reaction mixtures were diluted with water and then extracted with ethyl acetate. The crude products were purified by column chromatography to give the corresponding inhibitors. Synthetic scheme of investigated inhibitors is given in scheme 4

and chemical structures, abbreviations, IUPAC name and analytical data of the synthesized compounds are given in Table 2.4.

Table 2.3:IUPAC name, molecular structure, molecular formula, melting point and analytical data of the studied DHPCs

IUPAC name and abbreviation of Inhibitor	Chemical Structure	Molecular formula, M.P. and analytical data
2,4-diamino-7-nitro-5-(phenylthio)-5H-chromeno[2,3-b]pyridine-3-carbonitrile (DHPC-1)		$C_{19}H_{13}N_5O_3S$ (mol. wt. 391.07); Yield: 78%, mp; 206-208 ^o C; FT-IR (KBr, cm^{-1}): 3558, 3438, 3324, 2961, 2863, 2256, 1668, 1551, 1446, 1253, 1184, 1036, 962, 862, 774, 672, 632; ¹ H NMR (300 MHz, DMSO- d_6) δ (ppm): 5.136, 6.387, 7.129-7.238, 7.215-7.393, 7.396-7.468, 7.834, 7.935-8.073
2, 4-diamino-5-(phenylthio)-5H-chromeno [2, 3-b] pyridine-3-carbonitrile (DHPC-2)		$C_{19}H_{14}N_4OS$, (mol. Wt. 346.08), Yield: 84%, mp; 214-216 ^o C; FT-IR (KBr, cm^{-1}):3571, 3426, 3312, 2947, 2852, 2238, 1573, 1456, 1262, 1179, 1022, 935, 892, 729, 635; ¹ H NMR (300 MHz, DMSO- d_6) δ (ppm): 5.117, 6.218, 6.83-6.936, 6.964-7.982, 7.126-7.238, 7.329-7.398, 7.846
2,4-diamino-7-hydroxy-5-(phenylthio)-5H-chromeno[2,3-b]pyridine-3-carbonitrile (DHPC-3)		$C_{19}H_{14}N_4O_2S$, (mol. Wt. 362.40), Yield: 68-70%, mp; 256-258 ^o C; FT-IR (KBr, cm^{-1}): 3658, 3554, 3368, 2942, 2876, 2264, 1556, 1433, 1228, 1152, 1045, 949, 873, 746, 578; ¹ H NMR (300 MHz, DMSO- d_6) δ (ppm): 5.124, 6.135, 6.693-6.789, 6.792-6.836, 7.264, 7.348-7.394, 7.862

Scheme 4:



Synthetic route of studied AAIs

Table 2.4: IUPAC name, molecular structure, molecular formula, and analytical data of AAI-1, AAI-2, and AAI-3.

IUPAC name and abbreviation	chemical Structure	molecular formula and analytical data
N-((1H-indol-3-yl)(phenyl)methyl)-N-ethylethanamine (AAI-1)		Yield: 76%; $\text{C}_{19}\text{H}_{22}\text{N}_2$ (mol. wt. 278.39), IR spectrum (KBr cm^{-1}): 3534, 2956, 2856, 2628, 1658, 1622, 1426, 1241, 1163, 968, 854, 827, 827, 812, 745, 654; $^1\text{H NMR}$ (300 MHz, DMSO-d_6) δ (ppm): 1.23, 2.43, 5.23, 6.97-7.11, 7.29-7.38, 7.63, 7.95, 10.65.
3-(phenyl(pyrrolidin-1-yl)methyl)-1H-indole (AAI-2)		Yield: 86%; $\text{C}_{19}\text{H}_{20}\text{N}_2$ (mol. wt. 276.37), IR spectrum (KBr cm^{-1}): 3546, 3458, 2973, 2837, 2284, 1698, 1628, 1524, 1467, 1286, 929, 874, 837, 816, 763, 624 $^1\text{H NMR}$ (300 MHz, DMSO-d_6) δ (ppm): 1.73, 2.28, 5.36, 6.94-7.06, 7.18-7.26, 7.59, 7.96, 10.43
3-(phenyl(piperidin-1-yl)methyl)-1H-indole (AAI-3)		Yield: 87%; $\text{C}_{20}\text{H}_{22}\text{N}_2$ (mol. wt. 290.40), IR spectrum (KBr cm^{-1}): 3542, 3454, 2982, 2864, 2253, 1678, 1648, 1624, 1469, 1383, 1247, 987, 966, 893, 852, 823, 712, 643; $^1\text{H NMR}$ (300 MHz, DMSO-d_6) δ (ppm): 1.39-1.46, 2.42, 5.28, 6.88-6.94, 7.08-7.14, 7.74, 8.02, 10.63

2.3. Instruments and techniques

2.3.1. Characterization of the Synthesized Compounds

(i) Determination of melting point

Melting points of the synthesized compounds were determined in open capillaries using Reichert ThermoVar apparatus.

(ii) Spectroscopic characterization

Synthesized compounds were characterized using Infra-red (IR) and ¹H NMR spectroscopic methods. The IR spectra were recorded using Perkin Elmer (Spectrum100) Fourier transform (FT-IR) spectrophotometer whereas the ¹H NMR spectra at 300 MHz was recorded using the JEOL AL 300 FT-NMR in DMSO-D6 in which Tetramethylsilane (TMS) was used as internal standard.

2.3.2. Determination of corrosion rate and other related parameters

(i) Weight loss or gravimetric method: The cleaned, dried and accurately weighted mild steel specimens having dimension $2.5 \times 2.0 \times 0.025 \text{ cm}^3$ were immersed in 100 ml of 1 M HCl without and with different concentrations of inhibitors for 3 h. After the elapsed time, the specimens were removed, washed with distilled water and acetone, dried in moisture free desiccator. The clean and dry specimens were measured for the total surface area with utmost accuracy by using the following equation [ASTM (1990)]:

$$A = 2 (lb + lt + bt - \pi r^2 + \pi rt) \quad (1)$$

Where,

t = thickness of the specimen in cm

b = width of the specimen in cm

l = length of the specimen in cm

r = radius of the mounting hole

An electronic balance of high accuracy was used to measure the weight loss of the mild steel specimens before and after the experiments. To avoid any appreciable change in the corrosivity of the test solution during the weight loss study which may be due to exhaustion of corrosive constituents and/ or by accumulation of corrosion products that might cause further corrosion, the volume of test solution kept 100 ml [Mathur and Vasudevan (1982)]. After, elapsed time, the mild steel specimens were taken out, cleaned with distilled water, dried and weighted accurately with help of electronic balance of high accuracy. Form evaluated weight loss in the presence and absence of inhibitors, the corrosion rate (C_R), the percentage inhibition efficiency ($\eta\%$) and the surface coverage (θ) were calculated using following relationships [ASTM (1987)]:

$$C_R = \frac{87.6 \times w}{AtD} \quad (2)$$

$$\eta\% = \frac{C_R - C_{R(i)}}{C_R} \times 100 \quad (3)$$

$$\theta = \frac{C_R - C_{R(i)}}{C_R} \quad (4)$$

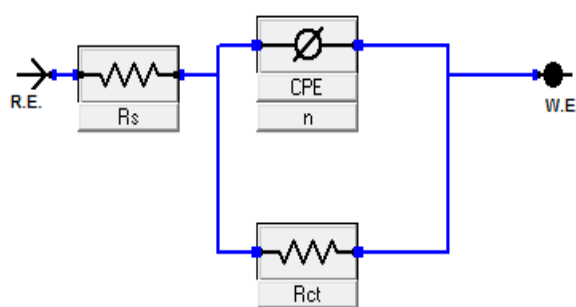
where, w is the weight loss of the specimen (mg), A the surface area of a specimen (cm^2), t exposure time (h) and D is the density of specimen (g cm^3). The C_R and $C_{R(i)}$ represent the corrosion rate in the absence and presence of inhibitors respectively.

(ii) Electrochemical measurement methods:

The mild steel specimens with exposed surface area of 1 cm² (one sided) was utilized for electrochemical measurements under potentiodynamic condition using the Gamry Potentiostat/Galvanostat (Model G-300) instrument. Gamry Echem Analyst 5.0 software was used to fit and analyze all electrochemical data. A three-electrode electrochemical cell consisting of mild steel as working electrode (WE), platinum as counter electrode and a saturated calomel electrode (SCE) as reference electrode was used for all the electrochemical measurements. All potentials were measured versus SCE.

(a) Electrochemical Impedance Spectroscopy

Electrochemical impedance measurements were carried out at the OCP in the frequency range of 100 kHz to 0.01 Hz using AC signal of amplitude 10 mV peak-to-peak. The values of charge transfer resistance (R_{ct}) were calculated using Nyquist plots obtained for inhibited and uninhibited solutions[Ashassi-Sorkhabiet *al.* (2008)]. The electrochemical impedance data were analyzed using an equivalent circuit model which physically represents the systems under investigation[Tao *et al.* (2011)]. The equivalent circuit used in my present case was previously described in literature and shown in below[Verma *et al.* (2015a)].



Equivalent circuit used in present study

The percentage inhibition efficiency ($\eta\%$) was calculated with the aid of values of R_{ct} in the absence and presence of inhibitors using the following equation:

$$\eta\% = \left(1 - \frac{R_{ct}}{R_{ct(i)}}\right) \times 100 \quad (5)$$

The values of C_{dl} for inhibited and uninhibited mild steel specimens can be calculated using the following equation:

$$C_{dl} = (Y_0 \cdot R_{ct}^{1-n})^{1/n} \quad (6)$$

where, Y_0 is CPE constant and n is a CPE exponent which can be used as a gauge of the heterogeneity or roughness of the surface.

(b) Potentiodynamic polarization technique

During polarization measurements, the cathodic and anodic Tafel slopes were recorded by changing the electrode potential from -0.25 to +0.25 V vs. corrosion potential (E_{corr}) at a constant sweep rate of 1.0 mV s⁻¹. The corrosion current density (i_{corr}) was determined by extrapolating the linear segments of the Tafel slopes (cathodic and anodic). The inhibition efficiency was calculated from the i_{corr} values by using the relation [ASTM (1994)]:

$$\eta\% = \frac{i_{corr}^0 - i_{corr}^i}{i_{corr}^0} \times 100 \quad (7)$$

where i_{corr}^0 and i_{corr}^i are corrosion current in the absence and presence of different concentrations of inhibitors, respectively.

2.4. Determination of Thermodynamic Parameters

(i) Determination of activation energy

While keeping all other parameters constant, the values of corrosion rate at different temperature ranging from 308 to 338 K was determined. The values of activation energy (E_a) were calculated from the slope of the plot of $\log(C_R)$ versus $1/T$ using the Arrhenius equation [Gupta *et al.* (2016)]:

$$\log(C_R) = \frac{-E_a}{2.303RT} + \lambda \quad (8)$$

(ii) Determination of Free Energy of Adsorption:

The free energy of adsorption of inhibitor at the metal surface was calculated using the equation given below [Weder *et al.* (2016)]:

$$\Delta G_{ads}^o = -RT \ln(55.5 K_{ads}) \quad (9)$$

Where, R is the gas constant, T is the absolute temperature, the numerical value 55.5 represents the concentration of water in acid solution and K_{ads} is the constant for adsorption desorption processes occurring over the metallic surface. The values of K_{ads} were calculated using following relationship [Ghareba and Omanovic (2010)]:

$$K_{ads} = \frac{\theta}{1-\theta} \times \frac{1}{C_{inh}} \quad (10)$$

Where, θ is the surface coverage and C_{inh} is the inhibitor concentration.

2.5. SEM, EDX and AFM measurements

For surface analysis, the cleaned mild steel specimens of above mentioned composition were allowed to corrode for 3h in absence and presence of optimum concentration of inhibitors. Thereafter, the specimens were taken out washed with water, dried and employed for SEM, EDX and AFM analysis. The SEM model Ziess Evo 50 XVP was used to investigate the micromorphology of mild steel surface at 500x magnification. Chemical composition of the inhibited and uninhibited specimens was recorded by an EDX detector coupled to the SEM. NT-MDT multimode AFM, Russia, 111 controlled by solvers canning probe microscope controller was employed for surface analysis by AFM method. The single beam cantilever having resonance frequency in the range of 240–255 kHz in semi contact mode with corresponding spring constant of

11.5N/m with NOVA programme was used for image interpretation. The scanning area during AFM analysis was 5 mm x 5 mm.

2.6. Computational studies

(a) Quantum chemical calculations

Quantum chemical calculations of the investigated compounds were carried out using the density functional theory (DFT) method involving the Becke three-parameter hybrid functional together with the Lee-Yang-Paar correlation functional (B3LYP) [Becke (1988); Lee *et al.* (1988); Becke (1993)]. The 6-31+G(d, p) basis set was chosen for all the calculations. The calculations were carried out with the aid of Gaussian 09 software for Windows (Revision D.01) [Frisch *et al.* (2009)]. The optimized geometries of the compounds were confirmed to correspond to their true energy minima by the absence of imaginary frequency in the computed vibrational frequencies. All quantum chemical parameters were derived based on the electronic parameters of the most stable conformers of the molecules. The frontier molecular orbital (FMO) energies, that is, the highest occupied molecular orbital energy (E_{HOMO}) and the lowest unoccupied molecular energy (E_{LUMO}) were calculated. Other parameters such as the energy gap (ΔE), global hardness (η), global electronegativity (χ), and the fraction of electrons transfer (ΔN) from the inhibitor to the metal atom were computed respectively according to the equations [Martinez (2003); Olasunkanmi *et al.* (2015)]

$$\Delta E = E_{LUMO} - E_{HOMO} \quad (11)$$

$$\eta = \frac{1}{2}(E_{LUMO} - E_{HOMO}) \quad (12)$$

$$\chi = -\frac{1}{2}(E_{LUMO} + E_{HOMO}) \quad (13)$$

$$\Delta N = \frac{\chi_{Fe} - \chi_{inh}}{2(\eta_{Fe} + \eta_{inh})} \quad (14)$$

where χ_{Fe} and η_{inh} denote the electronegativity and hardness of iron and inhibitor, respectively. A value of 7 eV/mol was used for the χ_{Fe} , while η_{Fe} was taken as 0 eV/mol for bulk Fe atom in accordance with the Pearson's electronegativity scale [Becke (1993)]. The total energy change (ΔE_T) that accompanies the donor-acceptor charge transfer process was calculated according to the approximation made by Gomez et al [Pearson (1988)]:

$$\Delta E_T = \frac{-\eta}{4} \quad (15)$$

where η was approximated to the chemical hardness of the inhibitor molecule. Selected dihedral angles that might have some correlations with the experimental inhibition efficiency of the compounds were also reported.

The Fukui functions f^+ and f^- are local reactivity indices that are often used to analyze the relative susceptibility of the active atomic sites of an inhibitor molecule to electrophilic and nucleophilic attacks respectively [Olasunkanmi *et al.* (2015); Gomez *et al.* (2006); Yan *et al.* (2013)]. The atom condensed Fukui functions using the Mulliken population analysis (MPA) and the finite difference (FD) approximations approach introduced by Yang and Mortier [Yang and Mortier (1986)] were calculated as:

$$f_k^+ = \rho_{k(N+1)}(r) - \rho_{k(N)}(r) \quad (16)$$

$$f_k^- = \rho_{k(N)}(r) - \rho_{k(N-1)}(r) \quad (17)$$

where f_k^+ and f_k^- are the electrophilic and nucleophilic Fukui indices respectively condensed on atom k , while $\rho_{k(N+1)}$, $\rho_{k(N)}$ and $\rho_{k(N-1)}$ are the electron densities of the $(N+1)$ -, (N) - and $(N-1)$ -electron systems respectively approximated by the Mulliken gross charges. The electron density surfaces of the f_k^+ and f_k^- were visualized using the Multiwfn software [Lu and Chen (2012a); Lu and Chen (2012b)].

(b) Molecular Dynamics (MD) Simulations

The molecular dynamics (MD) simulations were performed using Forcite module in the Material Studio Software 7.0 from BIOVIA-Accelrys, USA. Fe (110) surface was chosen for the simulation since it is the most stable crystal surface of Fe [Guo *et al.* (2014)]. The simulation was carried out with Fe (110) crystal with a slab of 5 Å in depth using periodic boundary conditions, in order to simulate a representative part of an interface devoid of any arbitrary boundary effects. The Fe (110) plane was then enlarged to a (8 × 8) supercell to provide a large surface for the interactions with the inhibitors. A vacuum slab of 30 Å thickness was then built above the Fe (110) plane. The Fe (110) surface was fixed before simulations. For the whole simulation procedure, the Condensed-phase Optimized Molecular Potentials for Atomistic Simulation Studies (COMPASS) force field was used to optimize the structures of all components of the system of interest. The MD simulations were performed in NVT canonical ensemble at 298K with applied settings of vdw& Coulomb, a cut-off radius of 15.5 Å, a time step of 0.1 fs and a total simulation time of 100 ps using Anderson thermostat. A total of 1,000,000 number of simulation steps were carried out.

The interaction energy ($E_{\text{interaction}}$) of molecules with Fe surface was obtained using the equation [Obot and Gasem (2014)]:

$$E_{\text{interaction}} = E_{\text{total}} - (E_{\text{Fe surface}} + E_{\text{molecule}}) \quad (18)$$

where E_{total} is the total energy of the molecules and the metal surface system; E_{surface} is defined as the energy of metal surface without adsorption of molecules and E_{molecule} is the energy of isolated molecules. The binding energy is the negative of the interaction energy and is given as:

$$E_{\text{binding}} = -E_{\text{interaction}} \quad (19)$$